The distinguishing effect of the magnetic states of cobalt on the performance of single-molecule magnet behaviors in a closely related $Co^{III}Dy^{III}$ and $Co^{II}Dy^{III}$ complexes

Anangamohan Panja,[a,b,*] Zvonko Jagličić,[c] Radovan Herchel,[d] Narayan Ch. Jana,[b] Paula Brandão[e] and Kuheli Pramanik[b]

[a] *Department of Chemistry, Gokhale Memorial Girls' College, 1/1 Harish Mukherjee Road, Kolkata-700020, India. E-mail: ampanja@yahoo.co.in*

[b] *Department of Chemistry, Panskura Banamali College, Panskura RS, WB 721152, India, India.*

[c] *Institute of Mathematics, Physics and Mechanics & Faculty of Civil and Geodetic Engineering, University of Ljubljana, Jadranska 19, 1000 Ljubljana, Slovenia*

[d] *Department of Inorganic Chemistry, Faculty of Science, Palacký University, 17. listopadu 12, 77146 Olomouc, Czech Republic*

[e] *Department of Chemistry, CICECO-Aveiro Institute of Materials, University of Aveiro, 3810-193 Aveiro, Portugal*

Table of Contents

Table S1. Crystallographic data and refinement details for **1** and **2**.

	1	**2**
Empirical formula	$C_{35}H_{42}N_4O_{15}CoDy$	$C_{47}H_{58}CoDyN_2O_{12.5}$
Formula weight	980.15	1072.38
Temperature/K	293(2)	150.00
Crystal system	triclinic	orthorhombic
Space group	$P\bar{1}$	Fdd2
a/Å	12.1528(4)	35.215(3)
b/Å	12.5134(4)	42.917(4)
c/Å	14.9487(5)	12.7391(9)
α/°	67.7210(10)	90
β/°	79.1420(10)	90
γ/°	66.4550(10)	90
Volume/Å^3	1926.63(11)	19253(3)
Z	2	16
ρ_{calc} g/cm^3	1.690	1.480
μ/mm^{-1}	2.430	1.947
F(000)	986.0	8752.0
2*Θ* range for data collection/°	5.9 to 55.262	4.434 to 54.374
Reflections collected	30619	8157
Independent reflections	8908 [R_{int} = 0.0331, R_{sigma} = 0.0321]	10400 [R_{int} = 0.0398, R_{sigma} = 0.0299]
Data/restraints/parameter	8908/0/529	10400/3/594
Goodness-of-fit on F^2	1.075	1.040
Final *R* indexes [I>=2σ (I)]	R_1 = 0.0244, wR_2 = 0.0572	R_1 = 0.0273, wR_2 = 0.0711
Final R indexes [all data]	R_1 = 0.0290, wR_2 = 0.0595	R_1 = 0.0314, wR_2 = 0.0734
Largest diff. peak/hole / e Å^{-3}	0.67/-0.87	1.18/-0.58

Table S2. Important bond distances (in Å) and angles (in deg.) of the structure **1** and **2**.

	1		**2**
Dy1– O3	2.2470(15)	Dy1– O1	2.377(3)
Dy1– O6	2.2780(15)	Dy1– O2	2.486(4)
Dy1– O7	2.4758(18	Dy1– O4	2.295(3)
Dy1–O8	2.5037(19)	Dy1–O5	2.610(4)
Dy1–O10	2.4857(19)	Dy1–O7	2.314(4)
Dy1– O11	2.5100(19)	Dy1– O8	2.396(4)
Dy1–O13	2.458(2)	Dy1–O9	2.425(4)
Dy1–O14	2.448(2)	Dy1–O10	2.471(4)
Dy1–O15	2.4311(17)	Dy1–O11	2.421(4)
Co1–O1	1.8970(15)	Co1–O1	2.078(3)
Co1–O3	1.9223(16)	Co1–O3	2.237(4)
Co1–O4	1.8965(15)	Co1–O4	2.003(4)
Co1–O6	1.9134(15)	Co1–O6	2.087(4)
Co1–N1	1.9241(19)	Co1–N1	2.064(4)
Co1–N2	1.9159(19)	Co1–N2	2.121(4)
Co1···Dy1	3.317(5)	Co1···Dy1	3.422(9)
Co1–O3–Dy1	105.14(7)	Co1–O1–Dy1	100.16(13)
Co1–O6–Dy1	104.28(7)	Co1–O4–Dy1	105.32(14)

Table S3. Shape analysis around cobalt center in **1** and **2**.

Label	**Shape**	**Symmetry**	**1**	**2**
HP-6	Hexagon	D_{6h}	32.839	31.703
PPY-6	Pentagonal pyramid	C_{5v}	27.818	24.598
OC-6	Octahedron	Oh	0.186	1.311
TPR-6	Trigonal prism	D_{3h}	14.741	10.612
JPPY-6	Johnson pentagonal pyramid J2	C_{5v}	31.744	27.776

Table S4. Shape analysis around Dy^{III} centers in **1** and **2**.

Label	**Shape**	**Symmetry**	**1**	**2**
EP-9	Enneagon	D_{9h}	36.151	35.949
OPY-9	Octagonal pyramid	C_{8v}	22.411	22.641
HBPY-9	Heptagonal bipyramid	D_{7h}	20.314	16.941
JTC-9	Johnson triangular cupola J3	C_{3v}	14.968	14.228
JCCU-9	Capped cube J8	C_{4v}	10.949	9.721
CCU-9	Spherical-relaxed capped cube	C_{4v}	9.591	8.354
JCSAPR-9	Capped square antiprism J10	C_{4v}	2.266	2.791
CSAPR-9	Spherical capped square antiprism	C_{4v}	1.327	1.689
JTCTPR-9	Tricapped trigonal prism J51	D_{3h}	3.741	3.730
TCTPR-9	Spherical tricapped trigonal prism	D_{3h}	2.092	2.392
JTDIC-9	Tridiminishd icosahedron J63	C_{3v}	11.142	11.430
HH-9	Hula-hoop	C_{2v}	10.857	10.369
MFF-9	Muffin	C_s	1.758	1.887

Table S5. Structural and magnetic features of 3d-4f complexes with ligand H_2L^1.[#]

Complex	nuclearity (topology)	Ln metal ion geometry	magnetic interaction	SMM, U_{eff}/K (Field)	Ref.
$[Ni_2Dy_2(HL^1)_2(\mu_3\text{-}OH)_2(piv)_6]\cdot 2CH_3CN$	Tetranuclear (butterfly)	TDD-8 (D_{2d})	weak	No	S1
$[Co_2Dy_2(HL^1)_2(\mu_3\text{-}OH)_2(piv)_6]\cdot 2H_2O$	Tetranuclear (butterfly)	TDD-8 (D_{2d})	weak	Yes, 40 K (5 kOe)	S1
$[Ni_2Dy_2(CH_3CO_2)_3(HL^1)_4(H_2O)_2]^{3+}$	Tetranuclear (arch-like)	BTPR-8 (C_{2v})	F	Yes, 19 K (0 kOe)	S2
$[Ni_2Tb_2(CH_3CO_2)_3(HL^1)_4(H_2O)_2]^{3+}$	Tetranuclear (arch-like)	JBCSAPR-10 (D_{4d})	F	Yes (2 kOe)	S2
$[Ni_2Ho_2(CH_3CO_2)_3(HL^1)_4(H_2O)_2]^{3+}$	Tetranuclear (arch-like)	JBCSAPR-10 (D_{4d})	F	-	S2
$[Ni_2Lu_2(CH_3CO_2)_3(HL^1)_4(H_2O)_2]^{3+}$	Tetranuclear (arch-like)	JBCSAPR-10 (D_{4d})	F	-	S2
$[NiGd(HL^1)_2(NO_3)_3]$	dinuclear	JBCSAPR-10 (D_{4d})	F	-	S2
$[NiGd(HL^1)_2(NO_3)_3]$	dinuclear	JBCSAPR-10 (D_{4d})	F	-	S3
$[NiPr(HL^1)_2(NO_3)_3]$	dinuclear	JBCSAPR-10 (D_{4d})	AF	-	S3
$[Ni_2La(HL^1)_4(NO_3)](NO_3)_2$	Trinuclear (linear)	JBCSAPR-10 (D_{4d})	AF	-	S3
$[Zn_2Gd(HL^1)_4(NO_3)](NO_3)_2$	Trinuclear (linear)	JBCSAPR-10 (D_{4d})	-	-	S3
$[Zn_2Pr(HL^1)_4(NO_3)](NO_3)_2$	Trinuclear (linear)	JBCSAPR-10 (D_{4d})	-	-	S3
$[Co_2Nd(HL^1)_4(NO_3)](NO_3)_2\cdot MeOH\cdot H_2O$	Trinuclear (linear)	In between JBCSAPR-10 (D_{4d}) and JSPC-10 (C_{2v})	AF	No	S4
$[Co_2Sm(HL^1)_4(NO_3)](NO_3)_2\cdot MeOH\cdot H_2O$	Trinuclear (linear)	In between JBCSAPR-10 (D_{4d}) and JSPC-10 (C_{2v})	F	Yes	S4
$[Co_2Gd(HL^1)_4(NO_3)](NO_3)_2\cdot MeOH\cdot H_2O$	Trinuclear (linear)	In between JBCSAPR-10 (D_{4d}) and JSPC-10 (C_{2v})	F	Yes	S4
$[Co_2Tb(HL^1)_4(NO_3)](NO_3)_2\cdot MeOH\cdot H_2O$	Trinuclear (linear)	In between JBCSAPR-10 (D_{4d}) and JSPC-10 (C_{2v})	AF	weak	S4
$[Co_2Dy(HL^1)_4(NO_3)](NO_3)_2\cdot MeOH\cdot H_2O$	Trinuclear (linear)	In between JBCSAPR-10 (D_{4d}) and JSPC-10 (C_{2v})	AF	weak	S4
$[Co_2La(HL^1)_4(NO_3)]\ (NO_3)_2$	Trinuclear (linear)	JSPC-10 (C_{2v})	AF	Yes, 10.65 K (1.5 kOe)	S5
$[Co_2Ce(HL^1)_4(NO_3)]\ (NO_3)_2$	Trinuclear (linear)	JSPC-10 (C_{2v})	AF	Yes, (5 kOe)	S5
$[Co_2Pr(HL^1)_4(NO_3)]\ (NO_3)_2$	Trinuclear (linear)	JSPC-10 (C_{2v})	AF	Yes, 15.03 K (2 kOe)	S5
$[Zn_2La(HL^1)_4(CH_3COO)](NO_3)_2$	Trinuclear (linear)	JSPC-10 (C_{2v})	AF	No	S6
$[Zn_2Ce(HL^1)_4(CH_3COO)](NO_3)_2$	Trinuclear (linear)	JSPC-10 (C_{2v})	AF	12.23 K (6 kOe)	S6
$[Zn_2Nd(HL^1)_4(CH_3COO)](NO_3)_2$	Trinuclear (linear)	JSPC-10 (C_{2v})	AF	No	S6
$[Zn_2Sm(HL^1)_4(CH_3COO)](NO_3)_2$	Trinuclear (linear)	JSPC-10 (C_{2v})	AF	No	S6
$[Zn_2Tb(HL^1)_4(CH_3COO)](NO_3)_2$	Trinuclear (linear)	JSPC-10 (C_{2v})	AF	No	S6
$[Zn_2Dy(HL^1)_4(CH_3COO)](NO_3)_2$	Trinuclear (linear)	JSPC-10 (C_{2v})	AF	Yes, 43.7 K (0 kOe), 88.63 K (2 kOe)	S6
$[Cu_2La(HL^1)_{4(}NO_3)](NO_3)_2$	Trinuclear (linear)	JSPC-10 (C_{2v})	AF	-	S7
$[Cu_2Ce(HL^1)_{4(}NO_3)](NO_3)_2$	Trinuclear (linear)	JSPC-10 (C_{2v})	AF	-	S7
$[Cu_2Pr(HL^1)_{4(}NO_3)](NO_3)_2$	Trinuclear (linear)	JSPC-10 (C_{2v})	AF	-	S7
$[Cu_2Gd(HL^1)_{4(}NO_3)](NO_3)_2$	Trinuclear (linear)	JSPC-10 (C_{2v})	F	-	S7
$[Cu_2Tb(HL^1)_{4(}NO_3)](NO_3)_2$	Trinuclear (linear)	JSPC-10 (C_{2v})	F	Yes, 15.7 K (0 kOe)	S7
$[Cu_2Dy(HL^1)_{4(}NO_3)](NO_3)_2$	Trinuclear (linear)	JSPC-10 (C_{2v})	F	Yes, 12.6 K (0 kOe)	S7
$[Cu_2Ho(HL^1)_{4(}NO_3)](NO_3)_2$	Trinuclear (linear)	JSPC-10 (C_{2v})	F	No	S7

Abbreviation: H_2L^1 = 2-[(2-hydroxymethyl-phenylimino)methyl]-6-methoxyphenol; piv = pivalate ion; F = ferromagnetic; AF = antiferromagnetic; TDD-8 = Triangular dodecahedron; BTPR-8 = Biaugmented trigonal prism; JBCSAPR-10 = Bicapped square antiprism; JSPC-10 = Sphenocorona

Table S6. Relaxation fitting parameters from the least-square fitting of the Cole-Cole plots of **1** by the single-component generalized Debye model with a double relaxation process at 2500 Oe dc fields.

T (K)	χ_S (emu/mol)	$\Delta\chi_2$ (emu/mol)	τ_2 (s)	α_2	$\Delta\chi_1$ (emu/mol)	τ_1 (s)	α_1
2	0.4201	1.61427	0.00273	0.46162	1.46545	0.35704	0.18387
2.15	0.40604	1.61905	0.00247	0.5028	1.37855	0.31439	0.14105
2.4	0.43828	1.63428	0.00179	0.51171	1.13012	0.25922	0.14373
2.6	0.45088	1.65116	0.00123	0.52216	0.96698	0.24083	0.13678
2.8	0.46675	1.62232	7.55E-04	0.51938	0.80547	0.20843	0.13617
3	0.43445	1.62579	4.39E-04	0.54071	0.67736	0.20114	0.1421
3.2	0.41567	1.64063	2.49E-04	0.55536	0.56403	0.18954	0.14286
3.4	0.24732	1.80808	9.73E-05	0.60348	0.46155	0.18607	0.12692
3.6	0	2.06387	2.68E-05	0.66133	0.36362	0.18372	0.09548
3.8	0	2.01649	1.29E-05	0.67115	0.30849	0.18309	0.08731
4	0	1.98775	6.30E-06	0.68915	0.24413	0.18588	0.10172
4.2	0	1.99849	2.17E-06	0.74205	0.16086	0.19748	0.05036

Table S7. Relaxation fitting parameters from the least-square fitting of the Cole-Cole plots of **2** by the single-component generalized Debye model with a double relaxation process at 2500 Oe dc fields.

T (K)	χ_S (emu/mol)	$\Delta\chi_2$ (emu/mol)	τ_2(s)	α_2	$\Delta\chi_1$ (emu/mol)	τ_1 (s)	α_1
2	0.34717	3.72599	5.24E-04	0.43148	1.22577	0.5569	0.1855
2.15	0.37038	3.66799	4.66E-04	0.4166	1.14676	0.52145	0.15161
2.4	0.41077	3.56483	4.31E-04	0.40068	0.99493	0.46705	0.16209
2.6	0.42748	3.48751	4.04E-04	0.39096	0.80982	0.42254	0.10621
2.8	0.44382	3.39269	3.84E-04	0.38357	0.68242	0.39722	0.08165
3	0.44758	3.28595	3.60E-04	0.37485	0.60306	0.39504	0.10756
3.2	0.48687	3.10606	3.41E-04	0.35369	0.55555	0.3357	0.09596
3.4	0.48898	3.03319	3.25E-04	0.34768	0.44995	0.32935	0.0628
3.6	0.52085	2.89105	3.14E-04	0.33329	0.3666	0.31327	0.01788
3.8	0.5498	2.75755	3.05E-04	0.32085	0.30762	0.30912	0.00397
4	0.54762	2.64465	2.88E-04	0.31304			
4.2	0.58312	2.51375	2.82E-04	0.2989			
4.4	0.56051	2.44492	2.62E-04	0.29708			
4.6	0.60236	2.29819	2.55E-04	0.2796			
4.8	0.6165	2.19653	2.42E-04	0.27029			
5	0.62243	2.10406	2.28E-04	0.26536			
5.5	0.64132	1.87824	1.90E-04	0.25008			
6	0.66567	1.67038	1.52E-04	0.24114			
6.5	0.7024	1.47387	1.19E-04	0.23283			
7	0.78485	1.2486	9.44E-05	0.23025			
7.5	0.87505	1.02857	7.48E-05	0.21488			
8	1.02388	0.7626	7.08E-05	0.17787			
8.5	1.054	0.63264	5.53E-05	0.17585			
9	1.09061	0.50455	4.32E-05	0.16515			
9.5	1.03793	0.47369	2.91E-05	0.16			
10	1.06784	0.36844	2.57E-05	0.13567			

Table S8. The splitting of the lowest multiplet for Dy^{III} ion in complex **1** calculated by CASSCF together with g-values for each Kramers doublet

E (cm^{-1})	g-factors		
0	0.085713	0.179411	19.291917
67	0.461335	0.758110	18.696931
134	1.541298	2.765583	14.077664
192	1.679237	7.239212	9.846448
222	1.510987	3.997197	13.483733
248	0.124309	7.350381	9.388703
258	0.529038	5.619413	11.565601
342	0.076603	0.171388	18.317937

Table S9. The splitting of the lowest multiplet for Dy^{III} ion in complex **2** calculated by CASSCF together with g-values for each Kramers doublet

E (cm^{-1})	g-factors		
0	0.016465	0.020371	18.621414
80	0.742314	1.814317	15.030222
110	0.636363	1.583566	17.356539
185	2.401225	3.363951	12.267896
213	4.370648	5.193061	10.272567
242	0.690496	1.347943	13.168140
290	1.260243	1.833171	15.764480
453	0.019488	0.035359	19.574005

Table S10. Structural and magnetic features of Co-Dy complexes with various ligands.[#]

Complex	Geometry of Dy	magnetic interaction	SMM, U_{eff}/K (Field)	Ref.
$[Co^{II}(\mu\text{-}L^{1})(\mu\text{-}Ac)Dy^{III}(NO_3)_2]$	-	Ferromagnetic	Yes, 7.6K (1 kOe)	S8
$Co^{II}(bpy)Dy^{III}(H_2O)(CH_3\text{-}PhCOO)_5$	BTPR-8 (C_{2v})	antiferromagnetic	Yes, NA	S9
$Co^{II}(phen)Dy(H_2O)(CH_3\text{-}PhCOO)_5$	BTPR-8 (C_{2v})	Ferromagnetic	Yes, ~2K, (0 Oe)	S9
$[Co^{II}(L^{2})(MeOH)(ac)Dy^{III}(hfac)_2]$	–	Ferromagnetic	Yes, 17.0K (1 kOe)	S10
$[Co^{II}Dy^{III}(L^{3})(DBM)_3]\cdot 3.5CH_3CN$	TDD-8 (D_{2d})	Ferromagnetic	Yes, NA	S11
$[Co^{II}Dy^{III}(CN)_6(hep)_2(H_2O)_4]$	PBPY-7 (D_{5h})	–	Yes, 63 K (2 kOe)	S12
$[Dy^{III}\{Co^{II}(\mu\text{-}H_2L^{5})\}piv_2(OH_2)]ClO_4)$	–	antiferromagnetic	Yes, NA	S13
$[Co^{II}Dy^{III}(H_2L^{12})(CH_3OH)_2(NO_3)_2](NO_3)\cdot MeOH$	TD-10 (C_{2v})	ferromagnetic	Yes, (1kOe)	S14
$[Co^{II}(CH_3CN)(\mu\text{-}L^{15})(\mu\text{-}OAc)Dy^{III}(NO_3)_2]\cdot CH_3CN$	CSAPR-9 (C_{4v})	ferromagnetic	Yes, 12.3K (1kOe)	S15
$[Co^{II}Dy^{III}(L^{16})(\mu 2\text{-}OOCC(CH_3)_3)_4(CH_3OH)]\cdot 3CH_3OH$	MFF-9 (Cs)	antiferromagnetic	No	S16
$[Co^{II}Dy^{III}(H2L^{17})(NO^{3})^{3}](CH^{3}OH)^{2}$	JSPC-10 (C_{2v})	antiferromagnetic	No	S17
$[Co^{II}Dy^{III}(HL^{19})(L^{20})(\mu\text{-}piv)(piv)_2]\cdot 0.5H_2O$	CSAPR-9 (C_{4v})	ferromagnetic	Yes. 2.2K (1kOe)	This work
$[Co^{III}Dy^{III}(HL^{4})(AcO)_3(H_2O)_3]\cdot(AcO)(H_2O)_3$	CSAPR-9 (C_{4v})	–	Yes, 113 K (2 kOe)	S18
$[Co^{III}Dy^{III}(L^{6})(\mu\text{-}OAc)_2(NO_3)_2]$	–	–	Yes, 18K (1kOe)	S19
$[Co^{III}Dy^{III}(L^{7})(\mu\text{-}OAc)_2(NO_3)_2]$	–	–	Yes, NA	S19
$[Co^{II}Dy^{III}(L^{8})(OAc)(NO_3)_2(CH_3OH)]$	TCTPR-9 (D_{3h})	–	Not reported	S20
$[Co^{III}Dy^{III}(pao)_3(NO_3)_3]$	JTCTPR-9 (D_{3h})	–	No	S21
$[Co^{III}Dy^{III}(mepao)_3(NO_3)_3]$	TCTPR-9 (D_{3h})	–	Yes, 16K (600 Oe)	S21
$[Co^{III}Dy^{III}(phpao)_{3(}NO_3)_3]$	TCTPR-9 (D_{3h})	–	No	S21
$[Co^{III}Dy^{III}(NH_2pao)_3(NO_3)_3]\cdot 3MeOH$	TCTPR-9 (D_{3h})	–	No	S21
$[Co^{III}(H_{0.5}L^{9})Dy^{III}(DBM)_2(H_2O)](ClO_4)0.5\cdot 3H_2O$	SAPR-8 (D_{4d})	–	Yes, 88.9K (2 kOe)	S22
$[Co^{III}Dy^{III}Br_2(L^{10})(acac)_2]\cdot CH_2Cl_2$	BTPR-8 (C_{2v})	–	Yes, 167K (0 kOe) Yes, 157K (1.5 kOe)	S23
$[Co^{III}Dy^{III}Cl_2(L^{11})(acac)Cl(MeO)]$	BTPR-8 (C_{2v})	–	Yes, 118K (0 kOe) Yes, 130K (1.5 kOe)	S23
$[Co^{III}Dy^{III}Cl_2(L^{11})(acac)Cl(H_2O)]$	BTPR-8 (C_{2v})	–	Yes, 70K (0 kOe) Yes, 128K (1.5 kOe)	S23
$[Co^{III}Dy^{III}Cl_2(L^{11})NO_3)_2(MeO)]$	CSAPR-9 (C_{4v})	–	No	S23
$[Co^{III}Dy^{III}(CH_3CN)0.5(L^{13})3(NO_3)_3]$	–	–	Yes, ~2.58K (3kOe)	S24
$[Dy^{III}Co^{II}(L^{14})(NO_3)_3]\cdot H_2O$	JBCSAPR-10 (D_{4d})	–	No	S25
$[Co^{III}Dy^{III}(L^{18})(\mu\text{-}Piv)^2(\eta^1\text{-}Piv)^2(\eta^1\text{-}OHMe)^2]$	TDD-8 (D_{2d})	–	Yes, ~0.3K (0 Oe) Yes, 3.9K (588 Oe)	S26
$[Co^{III}Dy^{III}(L^{19})_2(NO_3)_2(MeOH)_2]$	CSAPR-9 (C_{4v})	–	Yes. 54.7K (1kOe)	This work

Abbreviations: **H_2L^1:** N,N′N′′-trimethyl-N,N′′-bis(2-hydroxy-3-methoxy-5-methylbenzyl)diethylene triamine (H2L); **bpy:** 2,2′-bipyridine; **phen**: 1,10-phenanthroline; **L^2**: N,N′-bis(3-methoxy-2-oxybenzylidene)-1,3-propanediaminato; **ac**: acetate; **hfac**: hexafluoroacetylacetonato; **H_2L^3:** N,N′-dimethyl-N,N′-(2-hydroxy-3-methoxy-5-methyl-benzyl)ethylenediamine; **DBM**− : anion of 1,3-diphenyl-propane-1,3-dione; **H_3L^4**: 6,6'-((2-hydroxypropane-1,3-diyl)bis(azaneylylidene))bis(methaneylylidene))bis(2-methoxyphenol); **hep**: 1-(2-hydroxyethyl)-2-pyrrolidinone; **H_4L^5:** (1,4,7,10-tetraazacyclododecane-1,4,7,10-tetrayl)-tetrakis-(methylene)-tetrakis(2-methoxy-4-methylphenol); **L^6:** N,N′-ethylenebis(3-ethoxysalicylaldimine); **L^7:** N,N′-ethylenebis(3-methoxysalicylaldimine); **H_2L^8**: 1,2-bis(3-methoxysalicylideneaminooxy)ethane; **paoH**: 2-pyridinealdoxime; **mepaoH**: methyl 2-pyridyl ketone oxime; **phpaoH**: phenyl 2-pyridyl ketoneoxime; **NH_2paoH**: pyridine-2-amidoxime; **H_4L^9**: (2,2-[1,2-ethanediylbis[(hydroxyethylimino)methylene]]bis[6-methoxy-4-methyl-phenol]); **DBM**: dibenzoylmethane **H_2L^{10}**: N,N′-bis(2-oxy-3-methoxybenzylidene)-1,2-phenylenediamine; **H_2L^{11}**: N,N′-bis(2-oxy-3-methoxybenzylidene)-1,2-diaminocyclohexane; **H_4L^{12}**: 2,6-diacetylpyridinebis[2-(semicarbazono) propionylhydrazone]; **HL^{13}**: 8-hydroxyquinoline; **HL^{14}**: 3-methoxy-N-(2-(methylsulfanyl)phenyl)salicylaldimine); **H_2L^{15}**: N,N0-dimethyl-N,N0-bis(2-hydroxy-3-formyl-5-bromo-benzyl)ethylenediamine; **HL^{16}**: 1-(2-hydroxy-3-methoxybenzylidene)-semicarbazide; **H_4L^{17}**: *N*,*N*′,*N*′′,*N*′′′-tetra(2-hydroxy-3- methoxy-5-methylbenzyl)-1,4,7,10-tetraazacyclododecane; **H_2L^{18}:** N,N′ -bis(salicylidene)ethylenediamine. **H_2L^{19}**: 2-(((2-(hydroxymethyl)phenyl)imino)methyl)-6-methoxy-4-methylphenol; **L^{20}**: 2-(4H-benzo[d][1,3]oxazin-2-yl)-6-methoxy-4-methylphenol; BTPR-8 = Biaugmented trigonal prism; TDD-8 = triangular dodecahedron; PBPY-7 = Pentagonal bipyramid; TD-10 = Tetradecahedron; CSAPR-9 = Capped square antiprism; MFF-9 = Muffin-shape; JSPC-10 = Sphenocorona; TCTPR-9 = spherical tricapped trigonal prism; JTCTPR-9 = Tricapped trigonal prism (J51); SAPR-8 = square antiprism; JBCSAPR-10 = Bicapped square antiprism; NA = Not available.

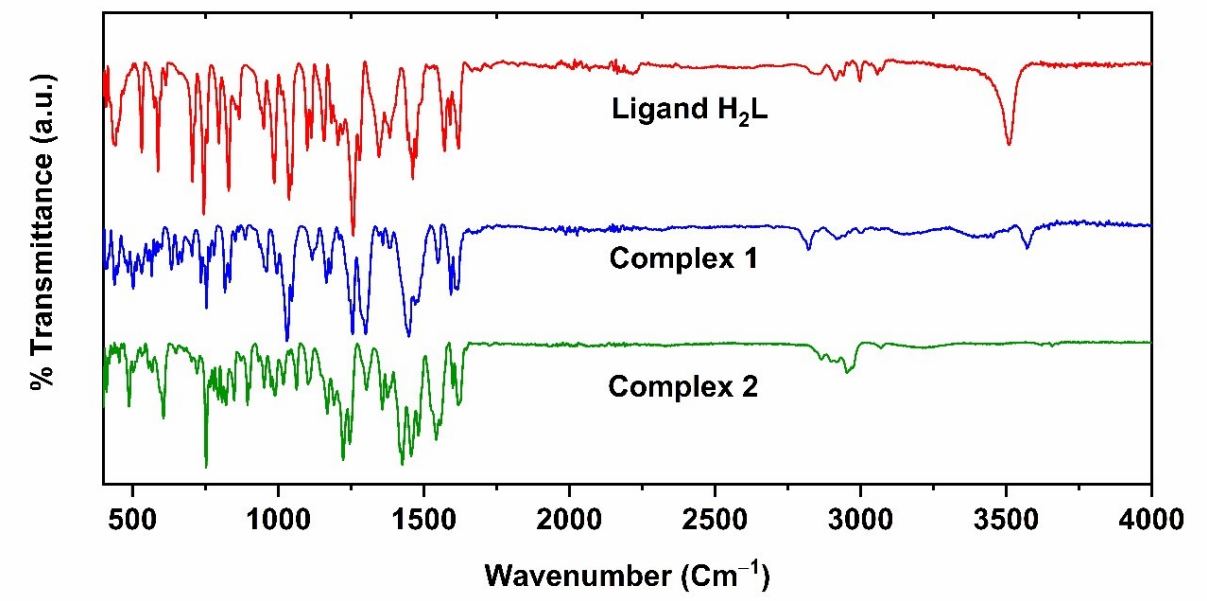

Fig. S1. IR spectra of Ligand H_2L and complexes **1** and **2**.

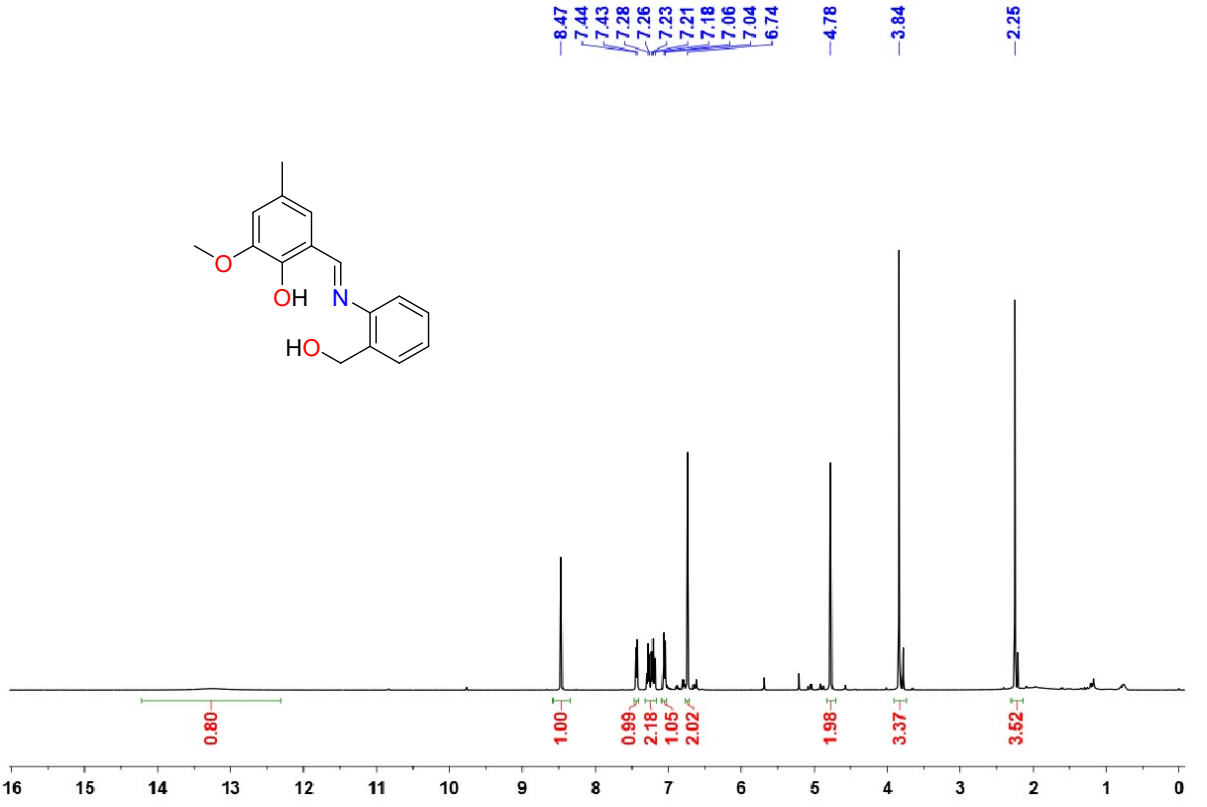

Fig. S2. ^{1}H-NMR spectrum of Schiff base H_2L in $CDCl_3$.

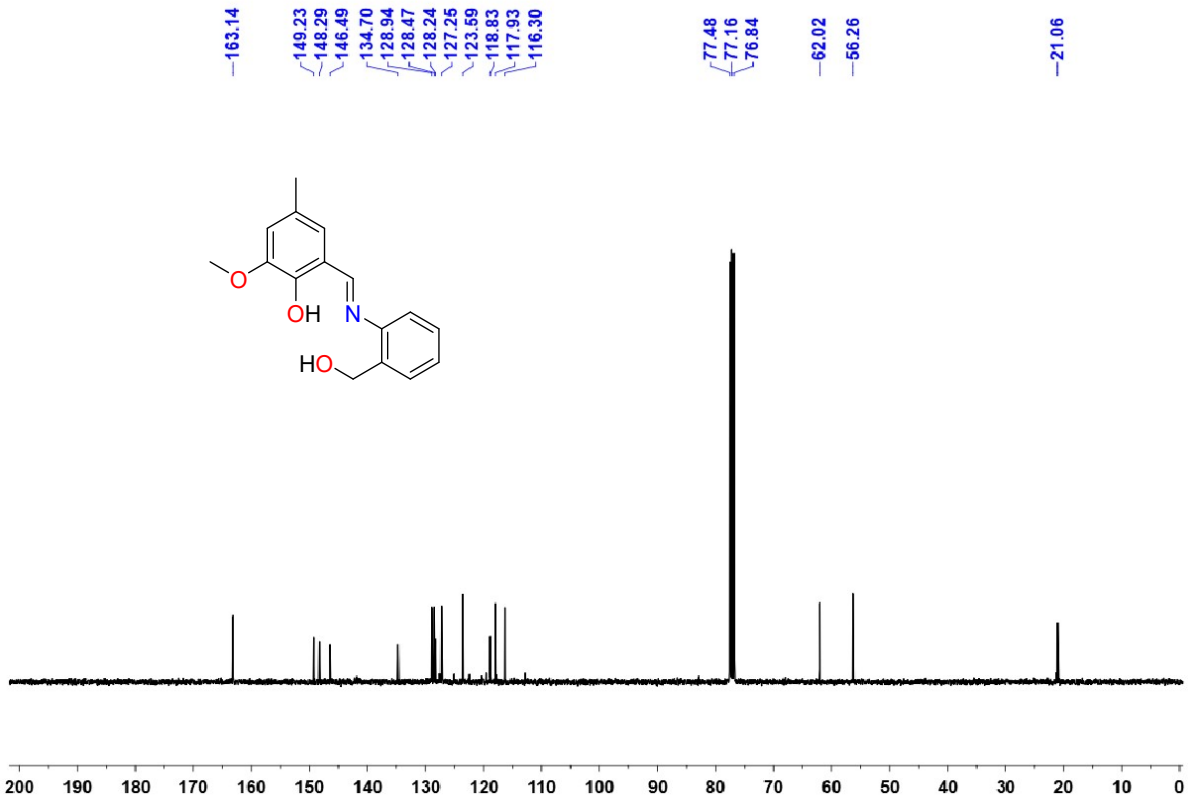

Fig. S3. ^{13}C-NMR spectrum of Schiff base H_2L in $CDCl_3$

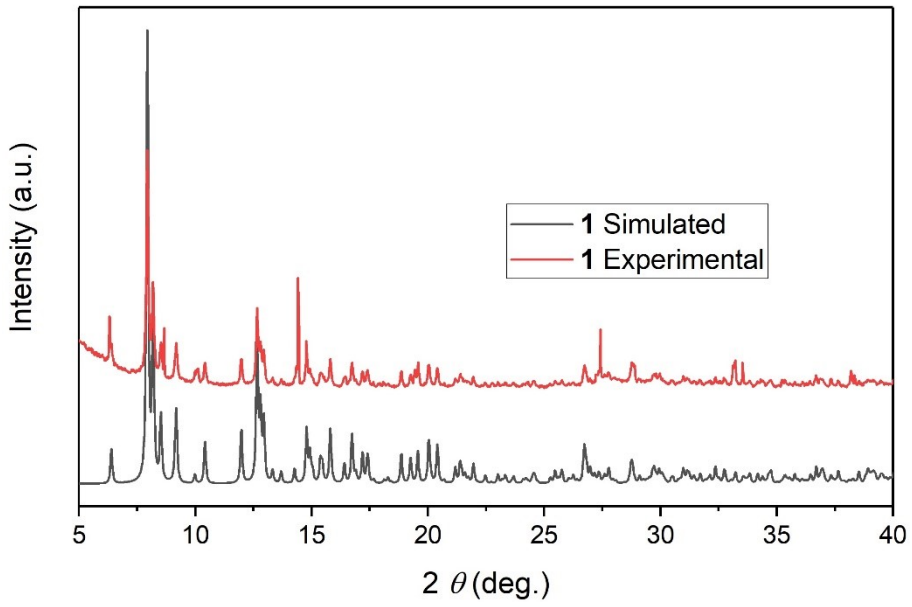

Fig. S4. PXRD data of complex **1**.

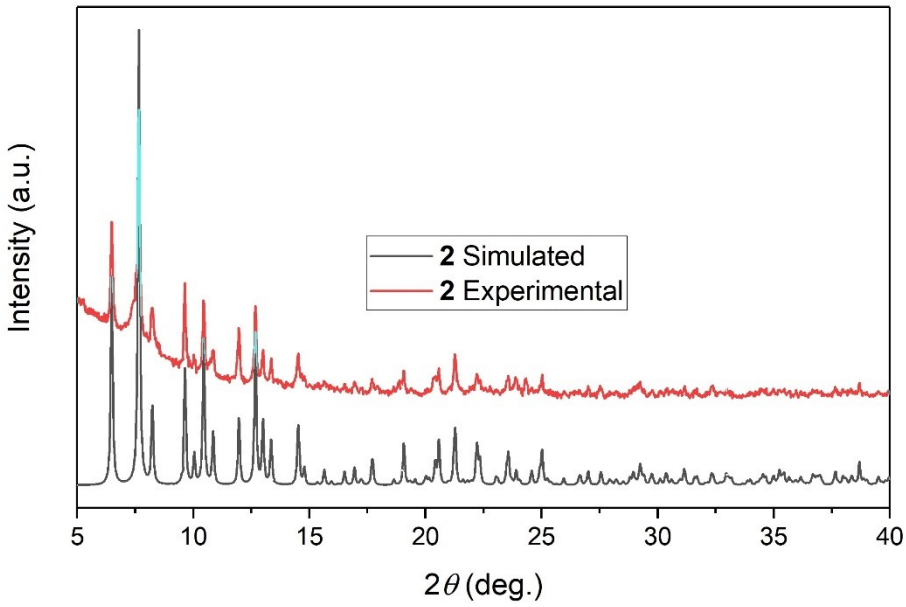

Fig. S5. PXRD data of complex **2**.

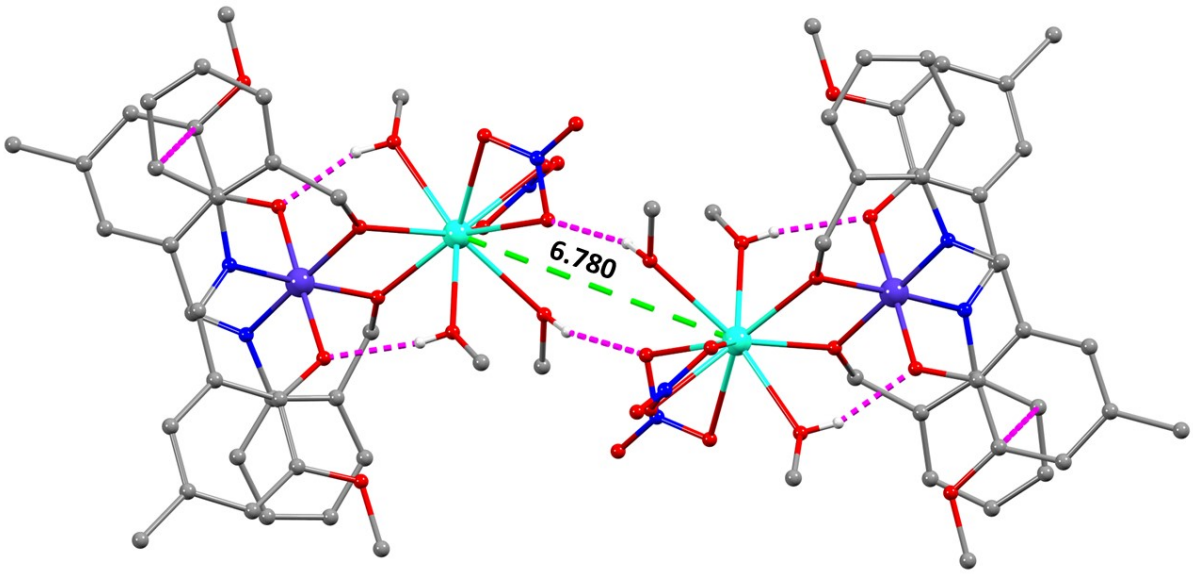

Fig. S6. A part of molecular packing of **1** showing different non-covalent interactions.

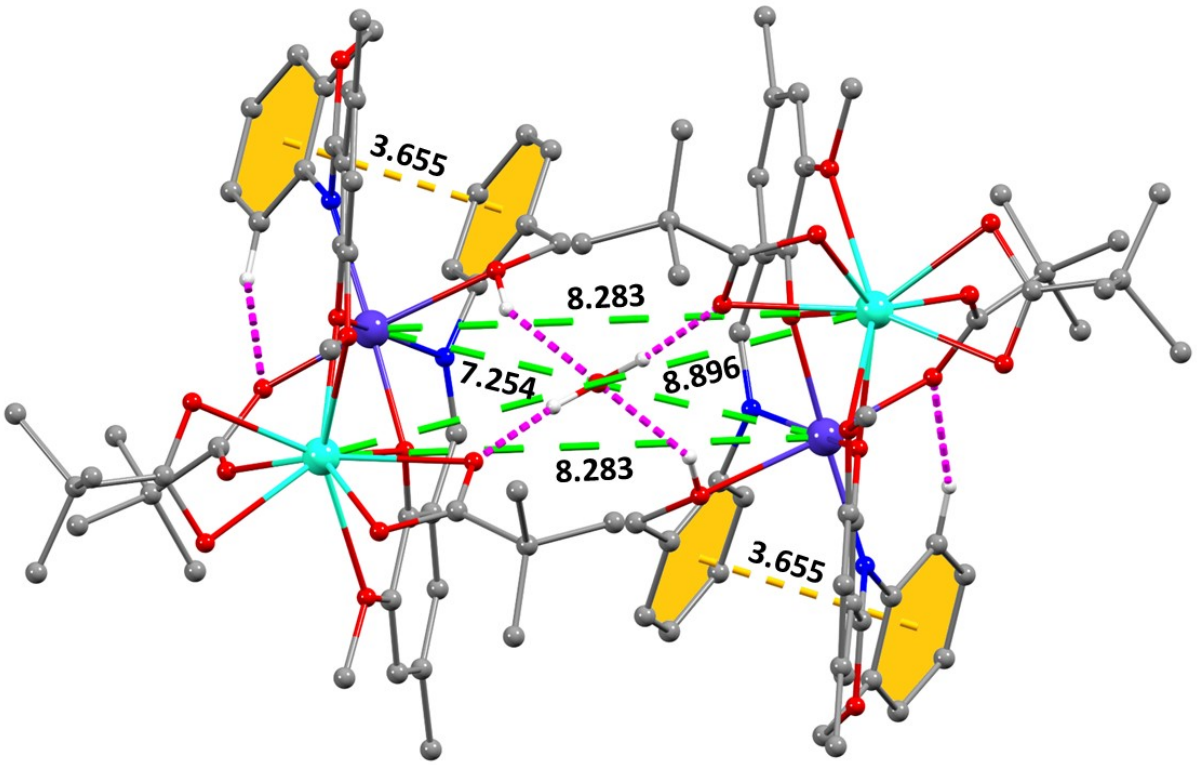

Fig. S7. A part of molecular packing of **2** showing different non-covalent interactions.

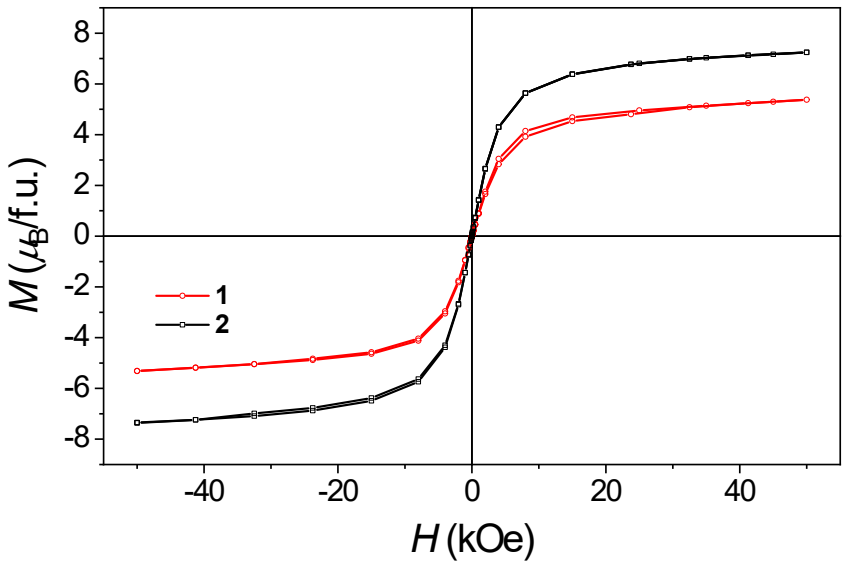

Fig. S8. Isothermal magnetization plots for **1** and **2** at 2 K.

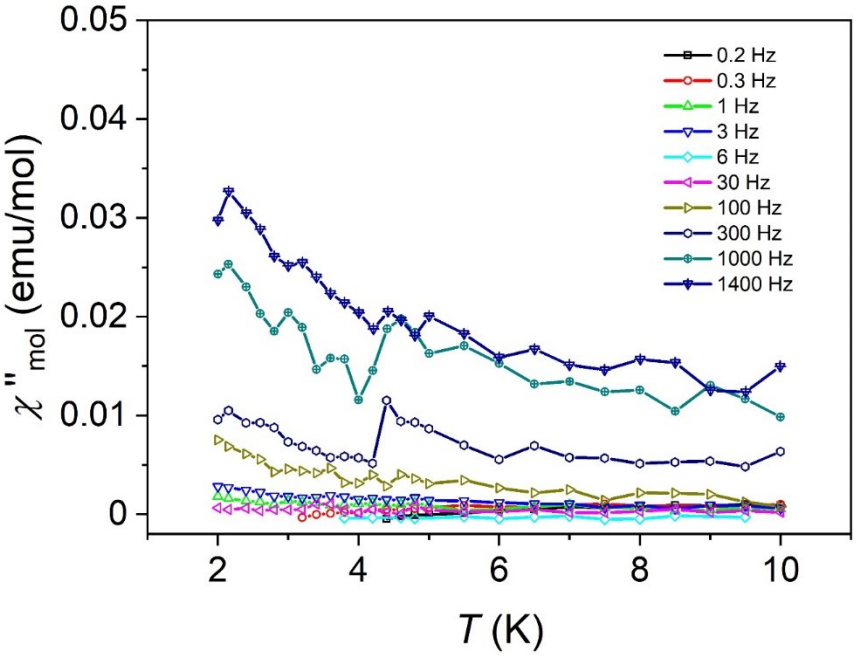

Fig. S9. Out-of-phase (χ″) ac susceptibility data for complex **1** at zero dc field.

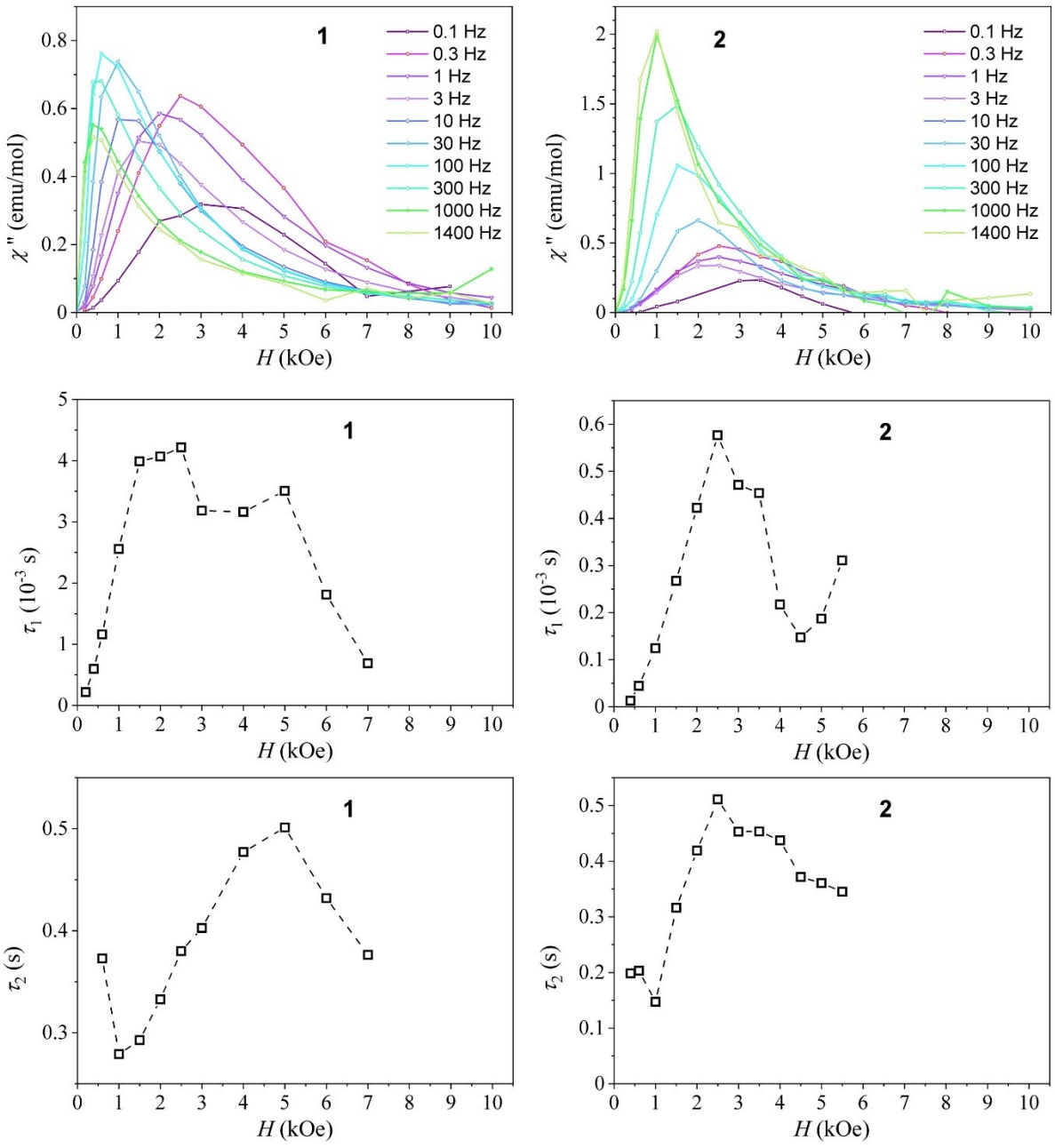

Fig. S10. The plots of χ'' as a function of applied magnetic field at 2 K and at selected ac frequencies, along with the plots of relaxation times (both τ_1 and τ_2) as a function of magnetic field for **1** and **2**.

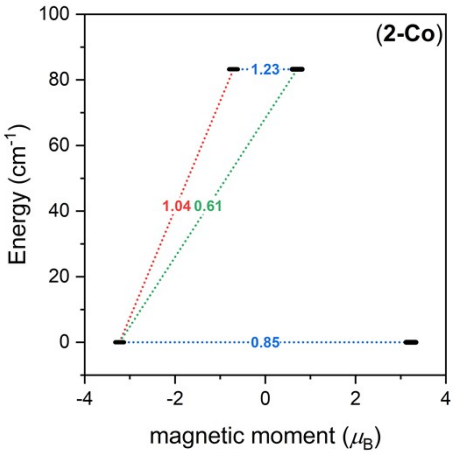

Fig. S11. The CASSCF/NEVPT2/SINGLE_ANISO calculations of ab initio magnetization blocking barrier for Co^{II} ion of **2**. The numbers presented in the plots represent the corresponding matrix element of the transversal magnetic moment (for values larger than 0.1 an efficient relaxation mechanism is expected).

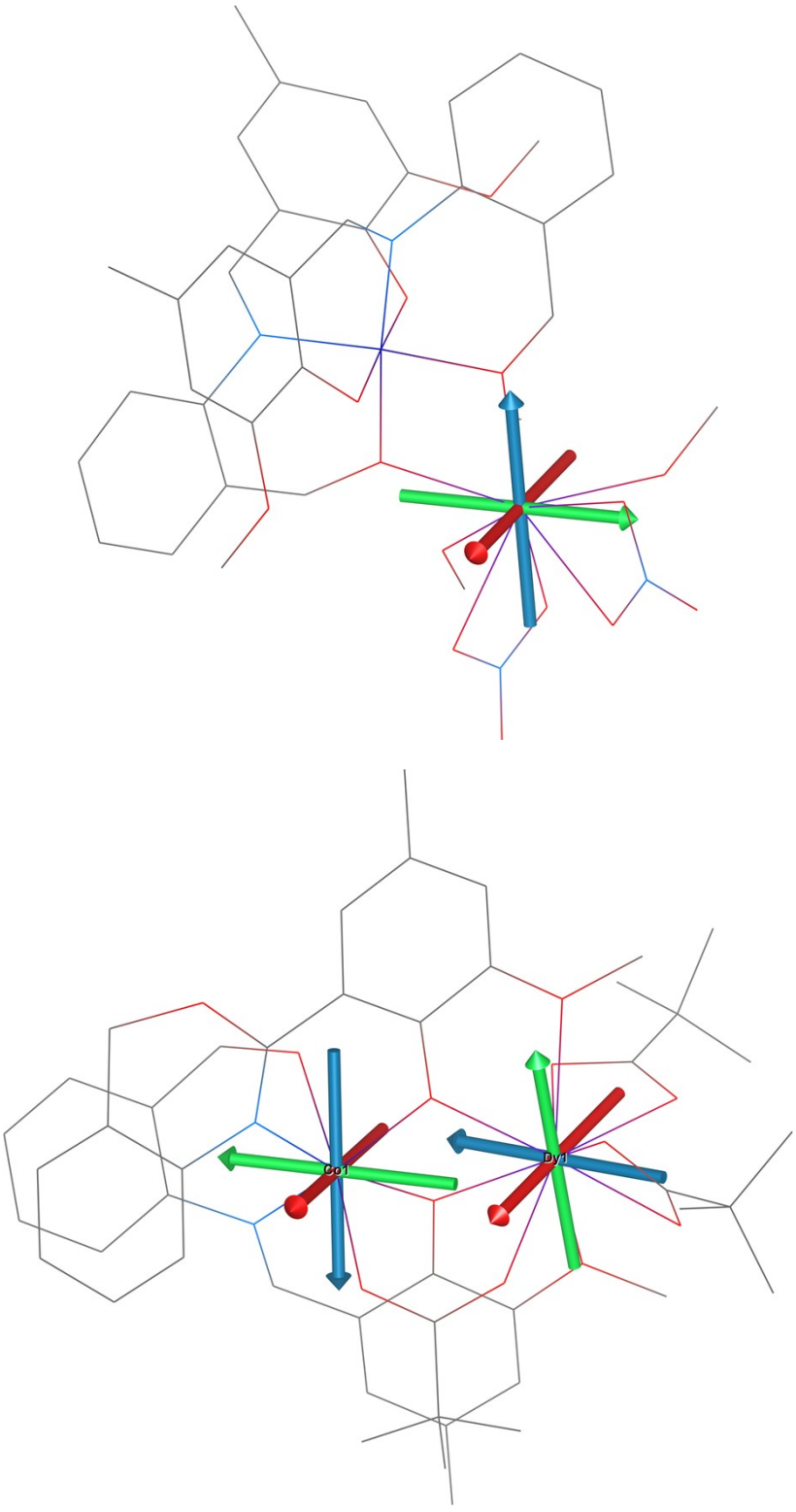

Fig. S12. The molecular structures of **1** (top) and **2** (bottom) overlaid with the principal axis of the *g*-tensor of the first Kramers doublet (x/y/z-axes colored as red/green/blue arrows) resulting from CASSCF/SINGLE_ANISO for Dy(III) ions and from CASSCF/NEVPT2/SINGLE_ANISO for Co(II) ion.

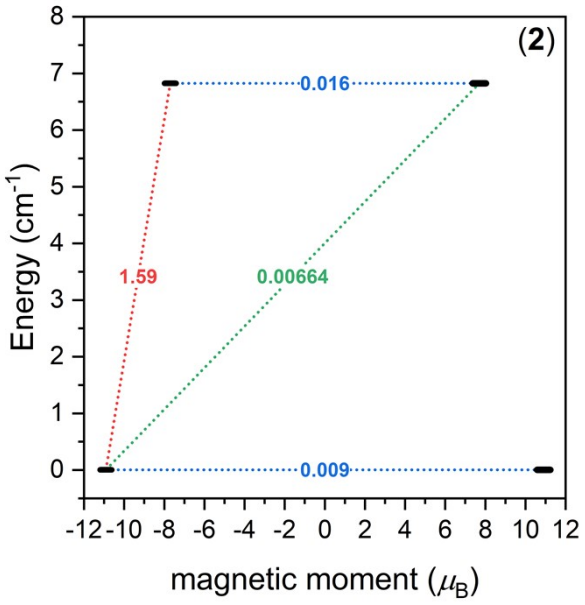

Fig. S13. The CASSCF/NEVPT2/POLY_ANISO calculations of ab initio magnetization blocking barrier for **2**. The numbers presented in the plots represent the corresponding matrix element of the transversal magnetic moment. The values colored in blue show the tunneling gap Δ_{tun} (cm^{-1}) of the indicated pseudo-doublets.

References

S1 N. C. Jana, A. Escuer, R. Herchel, J. Serra, R. Nandy and A. Panja, *Cryst. Growth Des*., 2024, **24**, 6492–6502

S2. N. Ahmed, C. Das, S. Vaidya, S. K. Langley, K. S. Murray and M. Shanmugam, *Chem. – Eur. J.*, 2014, **20**, 14235–14239.

S3. N. Ahmed, C. Das, S. Vaidya, A. K. Srivastava, S. K. Langley, K. S. Murray and M. Shanmugam, *Dalton Trans.*, **2014**, *43*, 17375–17384.

S4. R. Modak, Y. Sikdar, A. E. Thuijs, G. Christou and S. Goswami, *Inorg. Chem.*, 2016, **55**, 10192–10202.

S5. N. Ahmed and K. U. Ansari, *Dalton Trans.*, 2022, **51**, 4122–4134.

S6. N. Ahmed and K. U. Ansari, *Dalton Trans.*, 2022, **51**, 8766–8776.

S7. N. Ahmed, T. Sharma, L. Spillecke, C. Koo, K. U. Ansari, S. Tripathi, A. Caneschi, R. Klingeler, G. Rajaraman and M. Shanmugam, *Inorg. Chem.*, 2022, **61**, 5572–5587.

S8. E. Colacio, J. Ruiz, A. J. Mota, M. A. Palacios, E. Ruiz, E. Cremades, M. M. Hänninen, R. Sillanpää and E. K. Brechin, *C. R. Chim.*, 2012, **15**, 878–888.

S9. Y. Zhu, F. Luo, X.-F. Feng, Z.-W. Liao, Y.-M. Song, H.-X. Huang, X.-Z. Tian, G.-M. Sun and M.-B. Luo, Aust. J. Chem., 2013, 66, 75–83.

S10. M. Towatari, K. Nishi, T. Fujinami, N. Matsumoto, Y. Sunatsuki, M. Kojima, N. Mochida, T. Ishida, N. Re and J. Mrozinski, *Inorg. Chem.*, 2013, **52**, 6160−6178.

S11. Q.-W. Xie, S.-Q. Wu, W.-B. Shi, C.-M. Liu, A.-L. Cui and H.-Z. Kou, *Dalton Trans.*, 2014, **43**, 11309–11316.

S12. Y. Zhang, Z. Guo, S. Xie, H.-L. Li, W.-H. Zhu, L. Liu, X.-Q. Dong, W.-X. He, J.-C. Ren, L.-Z. Liu and A. K. Powell, *Inorg. Chem.*, 2015, **54**, 10316–10322.

S13. M. Bender, P. Comba, S. Demeshko, M. Großhauser, D. Müller and H. Wadepohl, *Z. Anorg. Allg. Chem.*, 2015, **641**, 2291–2299.

S14. F.-X. Shen, H.-Q. Li, H. Miao, D. Shao, X.-Q. Wei, L. Shi, Y.-Q. Zhang and X.-Y. Wang, *Inorg. Chem.*, 2018, **57**, 15526–15536.

S15. I. Oyarzabal, E. Echenique-Errandonea, E. San Sebastián, A. RodríguezDiéguez, J. M. Seco and E. Colacio, *Magnetochemistry*, 2021, 7, 22.

S16, M. Biswas, D. Basak, E. C. Sanudo and D. Ray, *New J. Chem.*, 2021, **45**, 8755–8762.

S17. Y. Jing, J. Wang, M. Kong, G.-Ji Wang, Y.-Q. Zhang and Y. Song, *Inorganica Chimica Acta* 2023, **546**, 121301.

S18. M. Dolai, M. Ali, J. Titiš and R. Boča, *Dalton Trans.*, 2015, **44**, 13242–13249.

S19. S. Hazra, J. Titiš, D. Valigura, R. Boča and S. Mohanta, *Dalton Trans.*, 2016, **45**, 7510–7520.

S20. W. K. Dong, J. C. Ma, Y. J. Dong, L. C. Zhu and Y. Zhang, *Polyhedron*, 2016, **115**, 228–235.

S21. C. D. Polyzou, E. S. Koumousi, Z. G. Lada, C. P. Raptopoulou, V. Psycharis, M. Rouzières, A. C. Tsipis, C. Mathonière, R. Clérac and S. P. Perlepes, *Dalton Trans.*, 2017, **46**, 14812–14825.

S22. M.-J. Liu, J. Yuan, B.-L. Wang, S.-T. Wu, Y.-Q. Zhang, C.-M. Liu and H.-Z. Kou, *Cryst. Growth Des.*, 2018, **18**, 7611−7617.

S23. J.-W. Yang, Y.-M. Tian, J. Tao, P. Chen, H.-F. Li, Y.-Q. Zhang, P.-F. Yan and W.-B. Sun, *Inorg. Chem.*, 2018, **57**, 8065–8077.

S24. P.P. Yang, S. Yu, L.X. Quan, H.C. Hu, D.C. Liu, Y.N. Liang, B. Li, F.P. Liang, and Z.L. Chen, *ChemistrySelect* **2020**, *5*, 9946–9951.

S25. D. Basak, J. van Leusen, T. Gupta, P. Kögerler, V. Bertolasi and D. Ray, *Inorg. Chem.*, 2020, **59**, 2387–2405.

S26. N. Barman, P. Halder, S, Mukhopadhyay, B. Schwarz, E. Colacio, R. Rana, G. Rajaraman, and J. Goura, New J. Chem., 2024, **48**, 15735–15746.